Defects induced in Yb3+/Ce3+ co-doped aluminosilicate fiber glass preforms under UV and γ-ray irradiation

(Article begins on next page)

25 April 2024

UNIVERSITÀ DEGLI STUDI DI TORINO

Defects induced in Yb^{3+}/Ce^{3+} co-doped aluminosilicate fiber glass preforms under UV and γ-ray irradiation

Mario Chiesa[a], Kent Mattsson[b], Stefano Taccheo[c], Thierry Robin[d], Laurent Lablonde[d], David Mechin[e], Daniel Milanese[f*]

[a]*Dipartimento di Chimica and NIS, Università di Torino, Via P.Giuria 7, I-10125 Torino, Italy*

[b]*NKT Photonics A/S, Blokken 84, DK-3460 Birkerød, Denmark / DTU Fotonik, Department of Photonics Engineering,*

[c]*College of Engineering, Swansea University, Singleton Park, Swansea SA2 8PP, UK*

[d]*iXFiber S.A.S., Rue Paul Sabatier, Lannion F-22300, France*

[e]*Perfos, R&D Platform of Photonics Bretagne, 11 rue Louis de Broglie, Lannion F-22300, France*

[f]*Institute of Materials Physics and Engineering, DISAT, Politecnico di Torino, Corso Duca degli Abruzzi 24, 10129 Torino, Italy;*

*corresponding author. Tel: +39 0110904707, Fax: +39 0110904699. Email: daniel.milanese@polito.it

Abstract:

A set of Ce- / Yb- co-doped silica optical fiber preform cores, differing in terms of dopants concentrations are studied by Electron Paramagnetic Resonance (EPR) spectroscopy before and after irradiation of the samples with excimer UV laser light and γ-rays. Evidence of Yb^{3+} clustering in the case of high Yb content samples is observed on as prepared samples regardless of the presence of Ce^{3+} ions. Si-E' and Al-OHC centers were identified upon photon irradiation. The results are correlated to the micro-structural origin of the photodarkening process occurring in Ce-Yb doped glass fibers.

1. Introduction

Yb-doped silica-based glasses are important materials for the fabrication of high power fiber lasers for materials processing [1]. However, a gradual increase of optical attenuation loss of the optical fiber cavity during laser operation, called photodarkening (PD), induces a decrease of the laser output power and creates hot spots in the laser systems which often leads to an accelerated ageing of the devices [2].

Several works have been carried out to study the dynamics of PD [3-6] and various mechanisms are proposed to explain the structural modifications of the glass materials underlying PD.

 The nature of dopant-related UV absorption bands are, however, still under debate [7]. A charge transfer transition between oxygen ligands and Yb^{3+} in formation of Yb^{2+} is discussed in [8] while Yb-related oxygen deficiency centers (ODCs) is proposed in [9] and a combination of both phenomena in [10].

Most researchers agree that PD is dependent on the occurrence and dimensions of Yb^{3+} ion clusters and some works explore the effect of photons either in the UV [8] or gamma ray [11] wavelength ranges and compared their effect on the irradiated glasses with the near infrared pump photons. One popular explanation for the mechanism of photodarkening comprise the generation of UV photons via multi-excitation of Yb clusters by IR pump radiation [13].

Photodarkening has been strongly reduced with the addition of co-dopants: P-codoping [14] or Ce [15]. The addition of P co-doping, however, influences other fiber parameters, such as an increase in background loss and a decrease of softening temperatures as well as emission and absorption cross sections. The Cerium ions appear to be a better choice as they allow a significant reduction of induced optical losses compared to P co-doping while retaining a positive effect on photodarkening [15].

The aim of this paper is to study a series of Ce-doped silica optical fiber preform cores, differing in terms of Yb concentration and co-dopants amount and ratio under parallel irradiation with photons in the UV and gamma ray wavelength regions. Defects are observed by Electron Paramagnetic Resonance (EPR) spectroscopy and compared with literature data concerning Ce-free glass materials. This paper brings for the first time to our knowledge evidence for that the degree of Yb^{3+} clustering is near to unaffected by the

presence of Ce ions. Further do the irradiation experiments using UV and gamma-ray sources demonstrate the occurrence of paramagnetic defects in all samples, regardless of the amount of Yb, Ce and Al dopants. These results add to the understanding of the mechanism of photodarkening and the applied method allow benchmarking different optical fibers without requiring the time consuming procedure of irradiation using near infrared pump photons.

2. Experimental procedure

2.1. Glass fabrication and Sample preparation

The set of core-cladding preforms are manufactured by the Modified Chemical Vapor Deposition (MCVD) process. The solution doping technique is employed to incorporate Al^{3+}, Yb^{3+} and Ce^{3+} ions and in order to avoid interference from possible defects induced in the cladding glass, this was mechanically removed using a lathe. The core cladding preforms prepared for this study are reported in Table 1, together with the correspondent values of Al/Yb and Yb/Ce weight ratio, and Yb concentration.

Table 1 – Preform samples employed for the current study.

Sample name	Al/Yb ratio	Yb/Ce ratio	Yb concentration $\times 10^{19}$ [ions/cm^3]
1271	5	1	8.3
1297	10	5	3
1305	10	2.5	3
1311	10	1	3
352	10	1	10

From each preform three slices are prepared: one slice is exposed to UV photons, a second slice to gamma rays and a third slice serves as reference. All preform slices are measured using EPR Spectroscopy before and after irradiation.

2.1 Irradiation test parameters

UV irradiation is carried out using a KrF excimer laser emitting at the wavelength of 248 nm with a pulse repetition rate and fluence of 200 Hz and 6 mJ/pulse, respectively. Each sample is irradiated with 200000 pulses.

Gamma rays from Cobalt-60 source are shot on the selected samples with a dose rate of 500 rad/h for a total of 2000 hours, corresponding to an overall irradiation of 1000 Krad.

2.2 EPR measurements

The measurements are performed in both the conventional Continuous Wave (CW) mode and Pulse mode. EPR experiments are performed on an ELEXYS 580 Bruker spectrometer (at the microwave frequency of 9.76 GHz) equipped with a liquid-helium cryostat from Oxford Inc. All experiments are performed at 10 K. The magnetic field is measured by means of a Bruker ER035M NMR gauss meter.

Electron-spin-echo (ESE) detected EPR experiments is carried out with the pulse sequence: $\pi/2- \tau- \pi- \tau-$echo, with microwave pulse lengths $t_{\pi/2} = 16$ ns and $t_\pi = 32$ ns and a τ value of 180 ns.

Hyperfine Sublevel Correlation (HYSCORE) [16] experiments is carried out with the pulse sequence $\pi/2- \tau- \pi/2 - t_1 - \pi- t_2 - \pi/2 - \tau-$ echo echo with the microwave pulse length $t_{\pi/2} = 16$ ns and $t_\pi = 16$ ns. The time intervals t_1 and t_2 are varied in steps of 16 ns starting from 96 ns to 5312 ns. A four-step phase cycle is used for eliminating unwanted echoes. The time traces of the HYSCORE spectra are baseline corrected with a third-order polynomial, apodized with a Hamming window and zero filled. After two-dimensional Fourier transformation, the absolute value spectra are calculated.

3. Results

3.1 EPR spectra on as made samples

The electron spin echo detected EPR (ESE-EPR) spectra for the different silica based core-cladding preforms are reported in Fig. 1 and 2. The ESE-EPR spectrum is recorded by measuring the transient signal generated by a two pulse sequence with fixed time interval and variable external magnetic field. In this way the signal absorption is measured directly, which is of considerable advantage with respect to

usual continuous wave EPR methods in the case of EPR spectra characterized by very broad lines. The spectra reported in Fig. 1 and 2 are characterized by broad resonance absorption signals that are characteristic of Yb^{3+} in silica based matrixes [17,18]. Yb^{3+} is a Kramers ion with $S=1/2$ for which a maximum theoretical g value $g=8$ can be expected, corresponding to a magnetic field of 87 mT at the operating frequency (9.76 GHz) [16]. All signals show, however, EPR absorption at zero field, which can only be explained considering the formation of Yb^{3+} clusters, as reported by ref. [18]. The signals for samples with lower Yb content, i.e. 1297, 1305 and 1311, are reported in Fig.1. They show a similar spectral pattern with absorption maxima between 430 and 470 mT, and a shoulder around 770 mT in addition to the zero-field absorption.
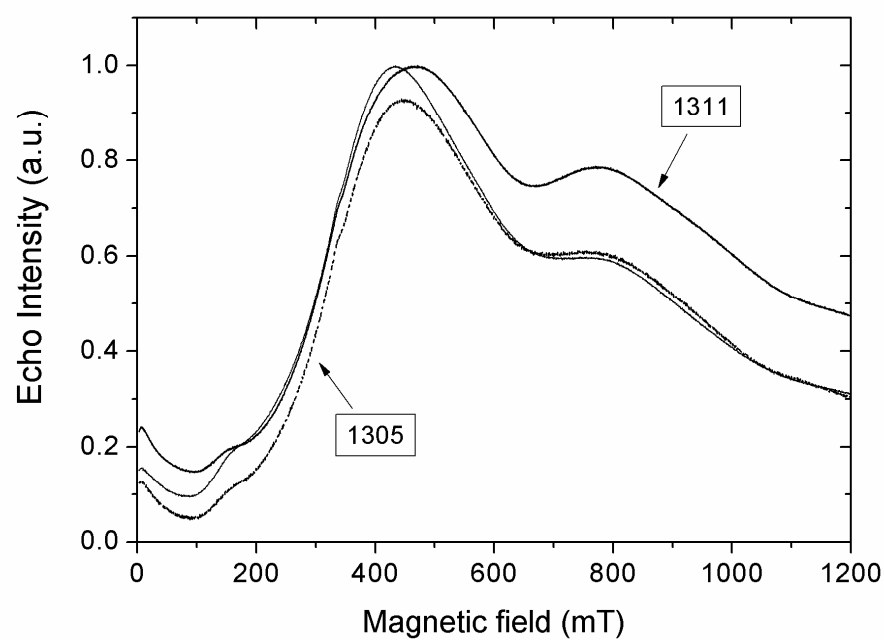
Figure 1 - Field-swept Yb3+ EDEPR spectra of pristine glass samples 1297, 1305 and 1311.

Different spectra are observed for the two samples with higher Yb content (1271 and 352 in Fig. 2) where a prominent absorption at approximately 800 mT is found. The samples also show an increased absorption at zero-field consistent with the high Yb content and consequent Yb clustering.

In Fig. 2 the ESE-EPR spectrum of Ce^{3+} in polycrystalline cerium titanate ($Ce_2Ti_2O_7$) is reported for comparison.

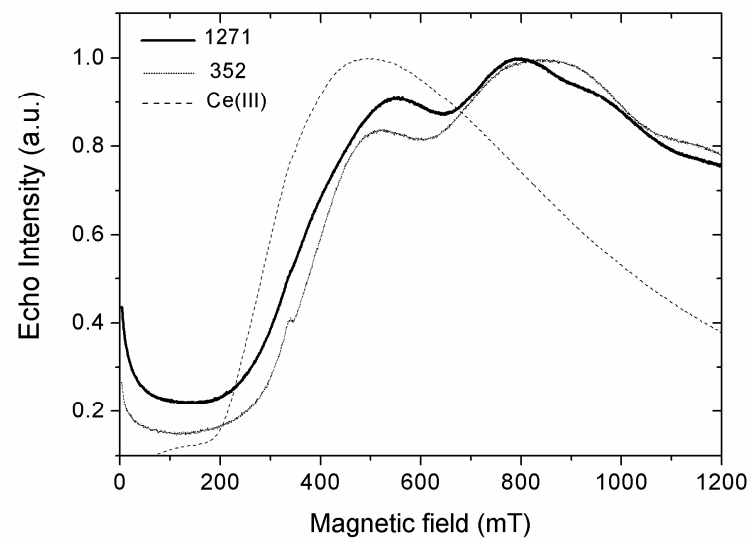**Figure 2 - Field-swept Yb³⁺ EDEPR spectra of pristine glass samples 1271 and 352. The spectrum of Ce³⁺ in polycrystalline Ce₂Ti₂O₇ is also reported (dotted line).**

In order to clarify the local environment of Yb^{3+} in the different systems, two-dimensional hyperfine sublevel correlation (2D-HYSCORE) EPR spectroscopy is performed. HYSCORE is a two-dimensional experiment where correlation of nuclear frequencies in one electron spin (m_S) manifold to nuclear frequencies in the other manifold is created by means of a mixing π pulse. The HYSCORE spectrum of sample 1305, recorded at a static magnetic fields of 500 mT and 800 mT is reported in Fig. 3. This is representative of the other samples.

The spectrum recorded at a magnetic field setting corresponding to the maximum absorption of the ESE-EPR spectrum (Fig. 3a) shows two peaks on the diagonal that are readily assigned to ^{29}Si and ^{27}Al neighboring nuclei based on the Larmor frequency. The peak relative to the ^{27}Al nucleus is slightly shifted with respect to the Larmor frequency due to the fairly large quadrupole interaction of ^{27}Al.
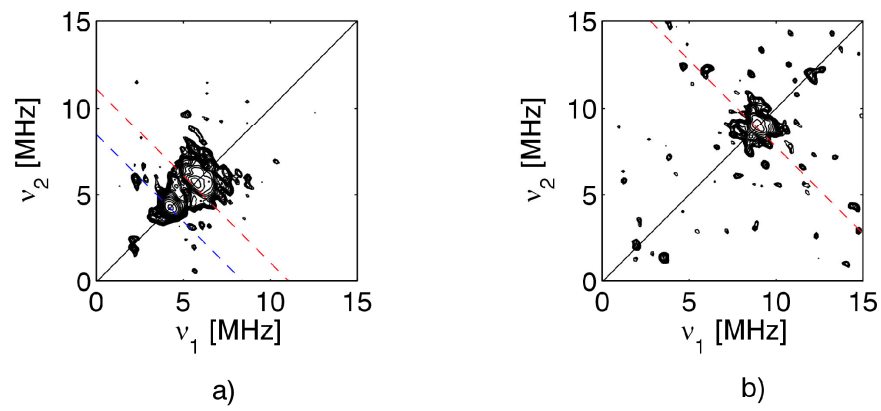
a)

b)

Figure 3 –2D-HYSCORE contour plot spectrum of the 1305 glass sample recorded at a static magnetic field of a) 500 mT and b) 800 mT and *t*=136 ns. The anti-diagonal dashed lines indicate the Larmor frequencies of [27]Al (red) and [29]Si (blue).

3.2 EPR spectra on irradiated samples

The effect of UV and gamma ray irradiation on the previously described samples is also tested. All samples show the onset of a new EPR signal at around 345 mT. In the case of UV irradiation the signal is weaker than for the γ-ray irradiated samples. A representative example is reported in Fig. 4, where a magnification of the overall signal is reported relative to sample 1305.

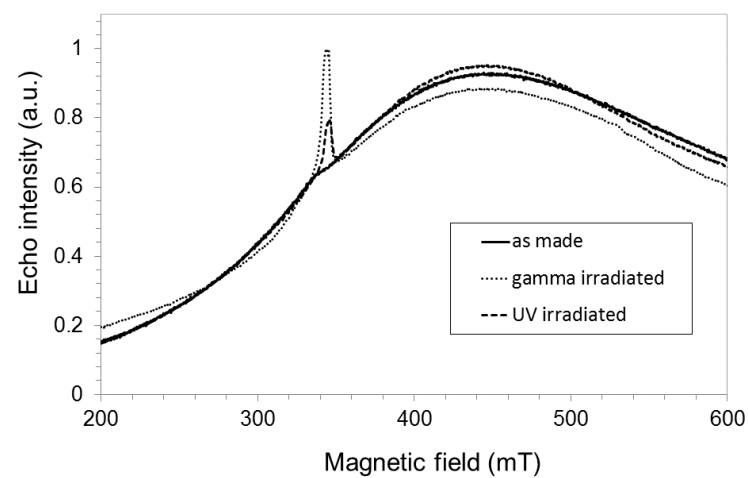**Figure 4 - Field-swept ESE-EPR spectra recorded at 10K of sample 1305: as made (continuous line), after irradiation with γ-rays (dotted line) and after UV irradiation (dashed line).**

While the overall shape and intensity of the broad signal associated to Yb[3+] centers is not affected by the different type of irradiation, the narrow signal resonating at 350 mT is more intense in the case of γ-ray

irradiation. The features of this relatively narrow spectrum are better detected operating in continuous wave mode. In Fig. 5 the CW-EPR spectrum of the defect generated by γ-ray irradiation is reported. Analogous spectra were obtained for the other samples.
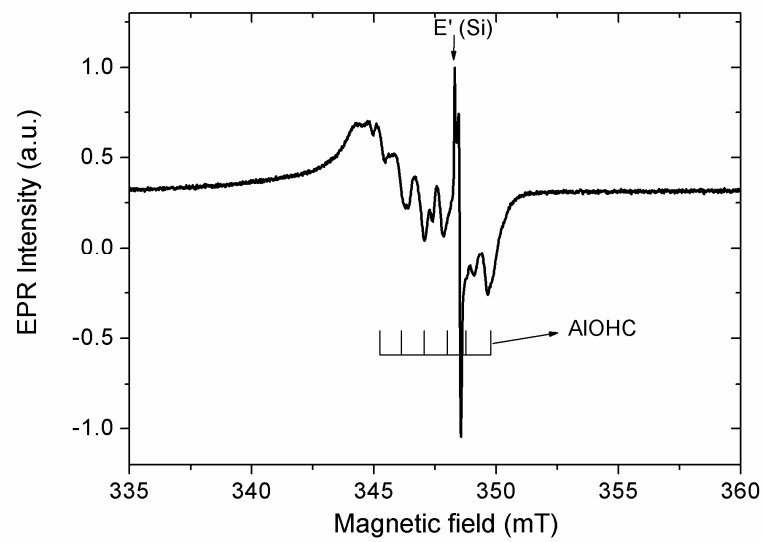
Figure 5 – CW EPR spectrum recorded at 10 K of the defect induced by γ-ray irradiation.

The spectrum is characterized by a complex powder pattern, which arises from the overlap of two distinct species associated to two different paramagnetic defects. A narrow axial line characterized by $g_\parallel$=2.002 and $g_\perp$=2.00 is associated to E'-Si centers [19]. This narrow signal is superimposed to a more complex pattern characterized by a 6-line multiplet characteristic of an Aluminum Oxygen Hole Center (AlOHC) defect [20].

4. Discussion

4.1 As prepared samples

Yb^{3+} has a $^2F_{7/2}$ ground state with 13 electrons in the 4f shell. Its configuration is thus equivalent to a single hole in the 4f shell. Yb^{3+} has been investigated in large number of crystals, especially those possessing octahedral site symmetry [21] where the ground state is a $|J_z=\pm1/2\rangle$ doublet with an isotropic g=2.667. The EPR spectra of the Yb^{3+} ion has also been observed in tetragonal site symmetry of $CaWO_4$

with the g values: $g_{\parallel}=1.058$, $g_{\perp}=3.92$ [22]. For Yb^{3+} in orthorhombic $ErBa_2Cu_3O_{7-\delta}$ and $YbBa_2Cu_4O_8$ the g-matrix values are $g_z=0.80$, $g_x=1.09$ $g_y=6.81$ and $g_z=1.40$, $g_x=2.48$ $g_y=5.5$, respectively [23].

The ESE-EPR spectra of all investigated samples (Fig. 1 and 2) are characterized by broad resonance absorptions extending from zero-field to 1200 mT. The spectra are consistent with results reported on the literature for Yb^{3+} species in glassy matrixes [17, 24]. In particular all spectra are characterized by absorption at zero-field zero, which can only be explained by the presence of Yb^{3+} clusters characterized by Yb-O-Yb bonds [18, 25]. The onset of Yb^{3+} clustering in GeO_2 glassy matrixes has been reported by Sen et al. [24] in the case of Yb^{3+} doping concentrations exceeding 3 x 10^{18} Yb^{3+}/cm^3. This is consistent with the relatively high concentration of Yb in our samples (see Tab. 1).

Samples 1271 and 352, containing a higher amount of Yb^{3+} ions, showed a higher peak intensity at zero-field, thus a correlation between the Yb concentration and clustering could be inferred. However a more reliable comparison is carried out by accurately weighing and measuring the same amount of glass for each sample.

As clear form the results, all Yb/Ce co-doped samples showed broad EPR spectra characteristic of Yb^{3+} species in glassy matrixes. In particular samples with low Yb content show a similar spectral pattern and they are similar to previously recorded spectra of Yb/Al silica glasses [18]. Similar signals are also observed for Yb/Al/P-doped silica preform samples [17]. A different spectrum is recorded in the case of highly Yb-doped glasses (Fig. 2): the increase in intensity of the band at around 800 mT is evident and is probably related to the Yb concentration, because it occurs both at low and high Al^{3+} ion content. The Yb/Ce ratio is the same for both samples, so there could be an effect also of the increased Ce concentration. The two samples with higher Yb content also have the highest Ce doping level. The possibility that Ce^{3+} is present in the glass can thus be invoked to explain the difference in the spectral features observed of spectra reported in Figures 1 and 2. In order to check for this possibility the spectrum of Ce^{3+} doped in a polycrystalline sample is reported for comparison (Fig. 2).

Ce^{3+} is a Kramers ion, similarly to Yb^{3+}, and its magnetic properties arise from the partially filled 4f shell [26]. The spectrum is characterized by a broad absorption resonance largely overlapping with the signal

due to Yb^{3+} species and is consistent with results for Ce^{3+} doped in silica glasses reported by Canevali et al. [27]. Although the spectrum of Ce^{3+} is characterized by a broad absorption resonance signal, largely overlapping with the Yb^{3+} spectrum, it does not account for the absorption maxima at approximately 800 mT observed in the glass preforms. This is in agreement with the similarity between the spectral patterns of our Ce doped samples and those of Yb^{3+} doped glasses reported in the literature [17, 18, 24]. It should be noted, however, that the EPR spectrum of both Yb^{3+} and Ce^{3+} is strongly dependent on the local symmetry, which governs the admixture of different Kramers doublets in the ground state, leading to a large variation in the **g** matrixes [28]. On the basis of these data we cannot thus exclude the presence of Ce^{3+}, although this analysis suggests that the main responsible for the spectral change is the degree of Yb clustering as well as the influence of the codopant (Ce) incorporated in excess, in modifying the structural sites occupied by Yb^{3+}.

In order to further characterize the local environment of Yb^{3+} species, HYSCORE spectra are recorded (Fig. 3), which reveal the super-hyperfine interaction with nearby ^{27}Al and ^{29}Si nuclei. The maximum extension of the ^{29}Si peak is approximately 2 MHz, in good agreement with the value reported by ref [18]. Assuming the Fermi contact term to be zero (a_{iso}=0) and assuming a pure dipole interaction [29] the Yb^{3+}-Si distance can be estimated to be of the order of 0.4 nm, consistent with the formation of Yb-O-Si bonds. Similar arguments hold also for the ^{27}Al signal, which indicates that Yb-O-Al units are also present. We note that at the other field position (Fig. 3b) the ^{29}Si signal is not present and a slightly reduced ^{27}Al ridge is observed. This may indicate that this shoulder in the ESE-EPR spectrum is due to different Yb^{3+} species, characterized by a different local environment. Given the low intensity of the spectra and the reduced modulation depth at this field (800 mT), it is not possible to obtain a firm evidence for this fact. This result did not differ with changing Yb content and Yb/Al or Yb/Ce ratios.

4.2 Irradiated samples

The results demonstrated that the effect of UV and γ-ray irradiation tests provided the same results in terms of paramagnetic defects produced, though the intensity of the so obtained signals in the case of UV irradiation was lower. In all cases the Yb^{3+} signal shape was not affected by the irradiation experiments.

The CW EPR experiments provided results in line with other works on Yb/P/Al doped silica glasses, where the occurrence of AlOHC was also recorded after γ-ray irradiation [11]. However in that case the presence of Ce^{3+} ions concealed the signal of Si(E') defects and Yb^{2+} formation was proposed as a possible electron trap. In this case the Si(E') centers were detected, even though this does not exclude the formation of Yb^{2+} ions, since Yb(II) is diamagnetic and cannot be detected by EPR spectroscopy.

Another work [30] reported the occurrence of similar defect centers in Al-doped silica VAD preform samples under gamma ray irradiation. However Si-E' and Al-OHC hole centers are reported along with an Al-E' electron trap center, which occurred in the 200 mT to 450 mT range. In this study the occurrence of the hyperfine structure of Al-E' signal could not be observed because it was possibly hindered by the wide absorption of the Yb^{3+} ion. Thus there is still the open question on the nature of the elctron trap: EPR spectroscopy does not detect diamagnetic centers, so a diamagnetic pathway cannot be excluded. The formation of Ce(III) from Ce(IV) or Yb(II) from Yb(III) could be another possibility, but no indirect evidence in the change of the amount of the paramagnetic ions (Ce(III) and Yb(III)) could be observed. Luminescence spectra were taken by exciting in the UV region both pristine and irradiated samples using a Perkin Elmer Perkin Elmer LS 55 fluorescence spectrometer, but no significant changes were observed after irradiation.

5. Conclusion

The investigation carried out allowed for the first time for the determination of the Yb^{3+} ion paramagnetic signal in a Ce-codoped silica glass used for manufacturing high power fiber lasers. The study of glass preform cores provide insight on the Yb^{3+} ion signal and allowed assessing clustering effects. Importantly the degree of Yb^{3+} clustering is found to be almost unaffected by the presence of Ce ions. This suggests

that the reduced photodarkening associated to the presence of Ce ions may have a different origin with respect to P doping, which has been demonstrated to inhibit Yb^{3+} clustering [17, 18]. Irradiation experiments using UV and γ-ray sources demonstrated the occurrence of paramagnetic defects in all samples, regardless of the amount of Yb, Ce and Al.

Further studies shall be focused on specific samples with controlled amount of dopants in order to study the limit of Ce doping and the benefit of Al^{3+} ions when Ce^{3+} ions are also introduced to mitigate photodarkening. A comparative study of Ce-free samples shall help in understanding the real benefit of this ion in terms of reduction of defects after irradiation.

Acknowledgments

References

[1] D.J. Richardson, J. Nilsson, and W.A. Clarkson, "High power fiber lasers: current status and future perspective", *J. Opt. Soc. Am. B*, vol. B27, pp. B63-B92, Nov. 2010. Doi: 10.1364/JOSAB.27.000B63.

[2] J. Koponen, M. Söderlund, H. Hoffman, and S. Tammela, "Measuring photodarkening from single-mode ytterbium doped silica fibers," Opt. Express 14 (2006) 11 539–11 544. Doi: 10.1364/OE.14.011539.

[3] S. Jetschke, S. Unger, U. Röpke, and J. Kirchhof, "Photodarkening in Yb doped fibers: experimental evidence of equilibrium states depending on the pump power", Optics Expr. 15, (2007) 14 838–14 843. Doi: 10.1364/OE.15.014838.

[4] J. Koponen, M. Söderlund, H.J. Hoffman, D.A.V. Kliner, J.P. Koplow, and M. Hotoleanu, "Photodarkening rate in Yb-doped silica fibers", Appl. Opt. 47 (2008) 1247-1256. Doi: 10.1364/AO.47.001247.

[5] S. Jetschke and U. Röpke, "Power-law dependence of the photodarkening rate constant on the inversion in Yb doped fibers", Opt. Lett. 34 (2009) 109-111. Doi: 10.1364/OL.34.000109.

[6] S. Taccheo, H. Gebavi, A. Monteville, O. Le Goffic, D. Landais, D. Mechin, D. Tregoat, B. Cadier, T. Robin, D. Milanese and T. Durrant, "Concentration dependence and self-similarity of photodarkening losses induced in Yb-doped fibers by comparable excitation", Opt. Expr. 19 (2011) 19340-19345. Doi: 10.1364/OE.19.019340.

[7] K. E. Mattsson, "Photo darkening of rare earth doped silica", Opt. Expr. 19 (2011) 19797-19812. Doi: 10.1364/OE.19.019797.

[8] S. Rydberg, M. Engholm, "Experimental evidence for the formation of divalent ytterbium in the photodarkening process of Yb-doped fiber lasers", Opt. Expr. 21 (2013) 6681-6688. Doi: 10.1364/OE.21.006681.

[9] S. Yoo, C. Basu, A.J. Boyland, C. Sones, J. Nilsson, J.K. Sahu and D. Payne, "Photodarkening in Yb-doped aluminosilicate fibers induced by 488nm irradiation", Opt. Lett. 32 (2007) 1626-1628. Doi: 10.1364/OL.32.001626.

[10] A.A. Rybaltovsky, A.A. Umnikov, K.K. Bobkov, D.S. Lipatov, A.N. Romanov, M.E. Likhachev,

V.B. Sulimov, A.N. Gur'yanov, M.M. Bubnov and E.M. Dianov, "Role of oxygen hole centres in the photodarkening of ytterbium-doped phosphosilicate fibre", Quantum Electron. 43 (2013) 1037-1042. Doi: 10.1070/QE2013v043n11ABEH015216.

[11] N. Ollier, R. Planchais, B. Boizot, "EPR study of Yb-doped irradiated glasses", Nucl. Instr. Meth. Phys. Res. B 266 (2008) 2854–2858. Doi: 10.1016/j.nimb.2008.03.129.

[13] J. Koponen, M. Söderlund, H. Hoffman, D. Kliner, and J. Koplow, "Photodarkening measurements in large mode area fibers," in Lasers and Applications in Science and Engineering. International Society for Optics and Photonics, 2007, pp. 64 531E–64 531E.

[14] A. Shubin, M. Yashkov, M. Melkumov, S. Smirnov, I. Bufetov, and E. Dianov, "Photodarkening of alumosilicate and phosphosilicate Yb-doped fibers" in Lasers and Electro-Optics, 2007 and the International Quantum Electronics Conference. CLEOE-IQEC 2007. European Conference on. IEEE, 2007, pp. 1–1. Doi: 10.1109/CLEOE-IQEC.2007.4386519.

[15] M. Engholm, P. Jelger, F. Laurell, and L. Norin, "Improved photodarkening resistivity in ytterbium-doped fiber lasers by cerium codoping", Opt. Lett. 34 (2009) 1285-1287. Doi: 10.1364/OL.34.001285.

[16] P. Höfer, A. Grupp, H. Nebenführ, M. Mehring, "Hyperfine sublevel correlation (hyscore) spectroscopy: a 2D ESR investigation of the squaric acid radical", Chem. Phys. Lett. 132 (1986) 279-282. Doi: 10.1016/0009-2614(86)80124-5.

[17] T. Deschamps, N. Ollier, H. Vezin, and C. Gonnet, "Clusters dissolution of Yb3+ in codoped SiO2-Al2O3-P2O5 glass fiber and its relevance to photodarkening", J. Chem. Phys. 136 (2012) 0145031-0145034. Doi: 10.1063/1.3673792.

[18] S. Sen, R. Rakhmatullin, R. Gubaidullin and A. Pöppl, "Direct spectroscopic observation of the atomic-scale mechanisms of clustering and homogenization of rare-earth dopant ions in vitreous silica", Phys. Rev. B 74 (2006) 1002011-1002014. Doi: 10.1103/PhysRevB.74.100201.

[19] D.L. Griscom "E' Center in Glassy SiO_2: Microwave saturation properties and confirmation of the primary [29]Si Hyperfine Structure", Phys. Rev. 20 (1979) 1823-1824. Doi: 10.1103/PhysRevB.20.1823

[20] D. L. Griscom, "Trapped-electron centers in pure and doped glassy silica: a review and synthesis," J.

Non-Cryst. Sol. 357 (2011) 1945–1962.

[21] W. Low and R.S. Rubins, "Evidence for Covalent Bonding from Electron Spin Resonance Spectra of Some Rare-Earth Ions in Single Crystals of Calcium Oxide", Phys. Rev. 131 (1963) 2527–2528. Doi: 10.1103/PhysRev.131.2527.

[22] U. Ranon and V. Volterra, "Paramagnetic Resonance of Yb^{3+} in $CaWO_4^{"}$, Phys. Rev. 134 (1964) A1483–A1485. Doi: 10.1103/PhysRev.134.A1483.

[23] S.K. Misra, Y. Chang and J. Felsteiner "A Calculation of Effective g-Tensor Values for R^{3+} Ions in $RBa_2Cu_3O_{7-\delta}$ and $RBa_2Cu_4O_8$ (R = Rare Earth): Low-Temperature Ordering of Rare-Earth Moments", J. Phys. Chem. Solids 58 (1997) 1-11. Doi: 10.1016/S0022-3697(96)00110-2.

[24] S. Sen, R. Rakhmatullin, R. Gubaydullin, A. Silakov, "A pulsed EPR study of clustering of Yb^{3+} ions incorporated in GeO_2 glass", Journal of Non-Crystalline Solids 333 (2004) 22–27. Doi: 10.1016/j.jnoncrysol.2003.09.051.

[25] B.M. Kozyrev, S.A. Al'tshuler, "Electron Paramagnetic Resonance in Compounds of Transition Elements", Wiley, New York, 1974, p. 589.

[26] S. K. Misra, S. Isber "EPR of the Kramers ions Er^{3+}, Nd^{3+}, Yb^{3+} and Ce^{3+} in $Y(NO_3)_3\cdot6H_2O$ and $Y_2(SO_4)_3\cdot8H_2O$ single crystals: Study of hyperfine transitions", Physica B Cond. Matt., 253 (1998) 111–122. Doi: 10.1016/S0921-4526(98)00373-1.

[27] C. Canevali ,M. Mattoni, F. Morazzoni, R. Scotti, M. Casu, A. Musinu, R. Krsmanovic, S. Polizzi, A. Speghini, M. Bettinelli "Stability of Luminescent Trivalent Cerium in Silica Host Glasses Modified by Boron and Phosphorus", J. Am. Chem. Soc., 127 (2005) 14681–14691. Doi: 10.1021/ja052502o.

[28] A. Abragam and B. Bleaney, "Electron Paramagnetic Resonance of Transition Metal Ions", Clarendon Press, Oxford, 1970.

[29] A. Pöppl and L. Kevan, "A Practical Strategy for Determination of Proton Hyperfine Interaction Parameters in Paramagnetic Transition Metal Ion Complexes by Two-Dimensional HYSCORE Electron Spin Resonance Spectroscopy in Disordered Systems", J. Phys. Chem. B 100 (1996) 3387. DOI: 10.1021/jp9525999.

[30] H. Hosono and H. Kawazoe, "Radiation-induced coloring and paramagnetic SiO$_2$:Al glasses", Nucl. Instrum. Meth. B 91 (1994) 395-399. Doi: 10.1016/0168-583X(94)96255-3.

Highlights:

- Pulse Electron Paramagnetic Resonance spectroscopy provides insight into the micro-structural origin of the photodarkening process occurring in Ce-Yb co-doped glass fibers.
- The degree of Yb3+ clustering is followed as a function of Yb and Ce doping and is found to be unaffected by the presence of Ce ions.
- Al-OHC and Si-E' paramagnetic centers are observed upon both UV and γ photoirradiation.